PROCEEDINGS OF SPIE

Investigation of the second hyperpolarizability of Ru-alkynyl complexes by z-scan and nonlinear scattering

Nick Van Steerteghem, Stijn Van Cleuvenbergen, Noor Aisyah Ahmad Shah, Mark G. Humphrey, Thierry Verbiest, et al.

SPIE.

Investigation of the second hyperpolarizability of Ru-alkynyl complexes by z-scan and nonlinear scattering

Nick Van Steerteghem[a], Stijn Van Cleuvenbergen[a], Noor Aisyah Ahmad Shah[b], Mark G. Humphrey[b] Thierry Verbiest[a], Koen Clays[a]

[a]Molecular Optics and Photonics, KU Leuven, Celestijnenlaan 200D, 3001 Heverlee, Belgium
[b]Research School of Chemistry, Australian National University, Canberra, ACT 2601 Australia

ABSTRACT

Present-day methods for determining the performance of third-order nonlinear optical materials include Z-scan, degenerate four-wave mixing and third-harmonic generation (THG). All these techniques possess severe drawbacks; for example, in THG, since all media (air and glass walls of the cell) present a third-order effect, eliminating these contributions requires careful, complex analysis or use of vacuum chambers. We have developed nonlinear scattering as a sensitive, straightforward technique for determining the second hyperpolarizability of samples in solution. Herein, we will for the first time show the applicability of the technique to measure organometallic Ru-complexes, optimized for high nonlinear responses. The investigated compounds showed a significant second hyperpolarizability $|\gamma|$, ranging from 1.1 for the least efficient to $2.8 \cdot 10^{-33}$ esu for the most efficient molecule, and comparable to fullerene C_{60} in thin films. It was deemed infeasible to extract hyperpolarizabilities using a high-frequency femtosecond laser source by a modified z-scan setup, which, in contrast to nonlinear scattering, could not account for the high degree of thermal lensing present in the investigated compounds.

Keywords: z-scan, nonlinear scattering, second hyperpolarizability, nonlinear refractive index, nonlinear optics

1. INTRODUCTION

Third-order nonlinear optics has a wealth of potential applications, including high-speed processing of data in photonic devices[1–3]. Along with inorganic semiconductors, organic materials are promising candidates, mainly because of their extreme ease of tailoring composition, courtesy of the recent advances in organic chemistry, allowing one to fine-tune the chemical structure to suit the exact needs of the nonlinear optical process at hand. An additional advantage worth mentioning explicitly is the fast response times in which organic materials respond to a given optical perturbation, allowing them to be used at the ever-increasing speeds at which devices are expected to work. These advantages underline the importance of determining the underlying structure-property relations of organic molecules for the different nonlinear processes. To this end, a fast, reliable experimental method to quantify the nonlinear optical properties, in particular third-order properties, is highly desirable. To date, the most widely-used methods, in no particular order, are: third-harmonic generation, electric field-induced second-harmonic generation, degenerate four-wave mixing, optical Kerr gate and z-scan. In this manuscript, we will, after a brief introduction, demonstrate the applicability of nonlinear scattering as a valid alternative experimental method, with significant advantages over all others, particularly in its ease of use, straightforward data analysis and sensitivity.

The induced dipole moment responsible for emission of radiation in nonlinear optical processes can be described by a Taylor-series expansion in powers of E:

$$\mu(\omega) = \alpha(\omega, t)E + \beta(\omega, t)E^2 + \gamma(\omega, t)E^3 + \cdots \quad , \qquad (1)$$

written in the so-called B-convention, which we shall adopt in the remainder of the manuscript. If instead of molecular properties the bulk properties of the material are described, the dipole moment μ is replaced by the dipole moment per unit volume P, and the polarizability α, first hyperpolarizability β and second

hyperpolarizability γ are replaced by the correct order susceptibilities, respectively $\chi^{(1)}$, $\chi^{(2)}$ and $\chi^{(3)}$. In Eq. (1), we explicitly wrote the time dependence of the molecular response to the applied electric field. Depending on the process responsible for the interaction with the incident electric field of the light, the time scale changes drastically. Fast processes, such as the polarization of electrons, referred to as the "electronic" part, have response times rarely longer than a few tens of femtoseconds. Slower processes range from hundreds of picoseconds in the case of polarization induced by atomic or molecular reorientation towards microseconds or milliseconds for light-induced heating of the material. For applications focused on exploiting the nonlinear refractive index, in order to achieve the high processing speeds in optical devices, the slow, thermal contributions need to be minimized while simultaneously maximizing the electronic part. However, quite detrimental is the fact that often thermal contributions are orders of magnitude larger than their electronic counterparts. This complicates matters when new materials are tested and their nonlinear optical properties measured. For example, when using high frequency, femtosecond pulsed laser sources, it is well known that thermal lensing completely dominates the self-(de)focusing effect induced by the electronic $\chi^{(3)}$.

2. RESULTS AND DISCUSSION

The ruthenium alkynyl compounds all show a characteristic low-lying metal-to-ligand charge-transfer excitation at around $20\,000\,\text{cm}^{-1}$ (Fig. 1). At higher energies, intra-ligand charge-transfer excitations become more important. The addition of a donor moiety in proceeding from molecule **1** to **2** has a subtle effect on the low-lying MLCT transition: a slight decrease in excitation energy and a slight increase in oscillator strength is observed. In contrast, the conjugation length of the individual ligands has a significant impact on the linear optical properties. In compounds **3** and **4**, even though they have the same number of electrons and empirical formula, molecule **3**, with a longer conjugated path length, has, unsurprisingly, a red-shifted absorption peak with a higher oscillator strength.
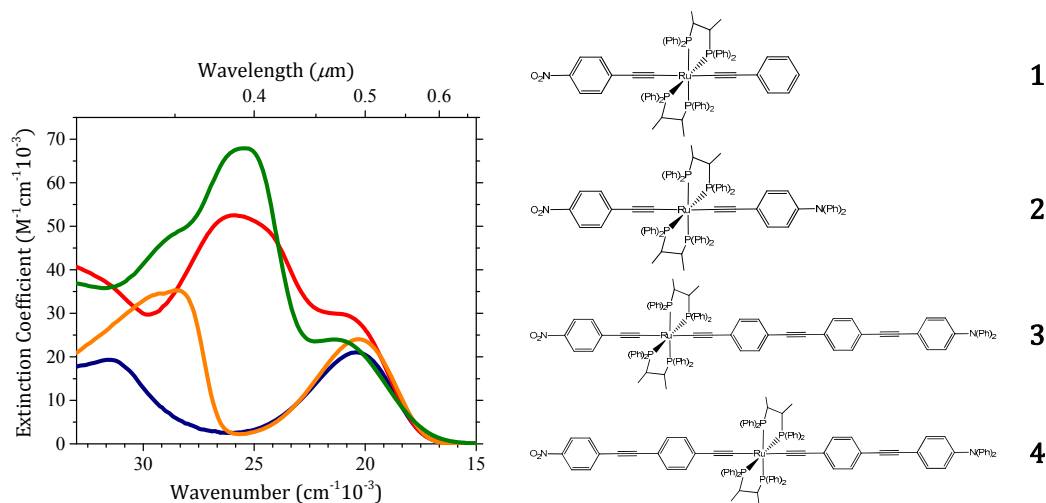
Figure 1. UV-VIS spectra of compound **1** (−, blue), compound **2** (−, orange), compound **3** (−, red) and compound **4** (−, green).

2.1 Z-scan

One of the most common techniques for probing second-order nonlinearities of compounds, z-scan is based on a self-action effect induced by the nonlinear refractive index n_2:

$$n(\omega) = n_0(\omega) + n_2(\omega)I \tag{2}$$

Self-focusing, self-defocusing and self-phase modulation are all phenomena that can be directly linked to n_2. In z-scan, the self-(de)focusing properties of the sample compound are exploited in order to extract the magnitude and sign of n_2[4]. By varying the position of a thin cuvette over the length (z-axis) of the laser beam and recording the transmittance in the far field, a peak-valley type curve is observed. The nonlinear refractive index n_2 can be related to the nonlinear susceptibility tensor[5]:

$$n_2(\text{m}^2\text{W}^{-1}) = \frac{120\pi^2}{n_0^2 c} \text{Re}\left(\chi_{iiii}^{(3)}(-\omega; \omega, \omega, -\omega)\right)(\text{esu}) \tag{3}$$

which in turn can be linked to the molecular second hyperpolarizability tensor $\langle\gamma(-\omega; \omega, \omega, -\omega)\rangle$, where the brackets denote an orientational averaging over all possible molecular orientations. The normalized transmission T of a closed-aperture z-scan trace is a well-known function[5] of the cell position z:

$$T = 1 - \frac{4\Delta\phi_0 v}{(1 + z^2/z_R^2)(9 + v^2)} \tag{4}$$

$$v = -\frac{1}{z_R}\left(z + \frac{z_R^2 + z^2}{z_1 - z}\right) \tag{5}$$

In order to avoid confusion, we will use the same notation as the authors of [5]. For clarity, z_r is the Rayleigh length, z_1 the distance to the detector and $\Delta\phi_0$ the nonlinear phase shift on the axis with the sample at the waist, equal to $2\pi/\lambda\, n_2 I_0 L$ in the absence of linear absorption.

When using high frequency, femtosecond pulsed laser sources, thermal lensing is a significant problem as the effect is usually several orders of magnitude larger than the self-(de)focusing induced by the electronic third-order susceptibility. We use a modified method of the z-scan technique[6], in which the input beam is modulated by a chopper; this enables the detection of a time dependent transmittance for which the thermal contribution can be separated from the electronic response. For the calibration of our z-scan setup, we measured the nonlinear refractive index of CS_2 by isolating the transmittance signal immediately after the chopper opening rise time (Fig. 2). We observed very similar behavior for the z-scan traces and the time dependent transmittance to that observed by the authors who proposed the technique [6,7] At a chopper frequency of 60 Hz, the signal rise time was equal to 25 μs, with the total chopper opening time equal to 250 μs, a down-time of 14.75 ms and a duty cycle of 1.7%. The result was a valley-peak type nonlinearity (indicating a positive n_2), measured immediately after the chopper opening rise time. Our result of $2.1 \cdot 10^{-15}$ cm^2/W (780 nm) agrees very well with the previously measured value of $2.3 \cdot 10^{-15}$ cm^2/W (770 nm) [6], taking into account the 10 nm difference in wavelength. Comparable values were measured using low repetition rate, short pulsed techniques, $3.10 \cdot 10^{-15}$ cm^2/W (800 nm), as well as techniques not related to z-scan ($2.50 \cdot 10^{-15}$ cm^2/W, 800 nm)[8]. However, at a higher duty cycle of 9%, the transmittance of CS_2 clearly had a significant contribution of a thermal component, evidenced by the reversal of the peak and valley in the z-scan curve. The measured value for n_2 of $-4.0 \cdot 10^{-15}$ cm^2/W indicates that 3 ms was insufficient time for complete normalization after the short irradiance period.

The time dependence of the transmittance in neat THF was of a much higher magnitude than that in neat CS_2. After approximately 250 μs, the transmittance decreased to less than 50% of its original value at some positions of the cuvette along the z-axis, and in particular at locations close to z_0. The same time-behavior was observed for compounds **1-4** dissolved in THF (Fig. 2), with a strong dependence on the concentration, indicating that the thermal effect is magnified at higher concentrations. The measured nonlinear refractive index for sample **1**, with

the transmittance recorded after 25 μs, still shows significant evidence of thermal contributions. Indeed, the negative value of $n_2 = -3.9 \cdot 10^{-15}$ cm^2/W for a $7.4 \cdot 10^{-3}$ mole/L solution is indicative of a thermal nonlinearity due to thermal self-defocusing in a medium with a negative temperature coefficient of the refractive index. The characteristic time of the thermal nonlinearity is evidently quite fast with respect to the chopper opening rise time, and, consequently, the transmittance at the earliest time where it can be measured already contains a significant thermal portion, dominating the purely electronic part of the nonlinear refractive index. In addition to the negative value for n_2, we observed a significantly increased separation in peak-to-valley distance, equal to $2.74 z_r$. These observations point towards thermal lensing originating from an absorption that is linear with respect to the incident intensity, which theoretically predicts a peak-to-valley separation of $2\sqrt{3} z_r = 3.46 z_r$[7,9].
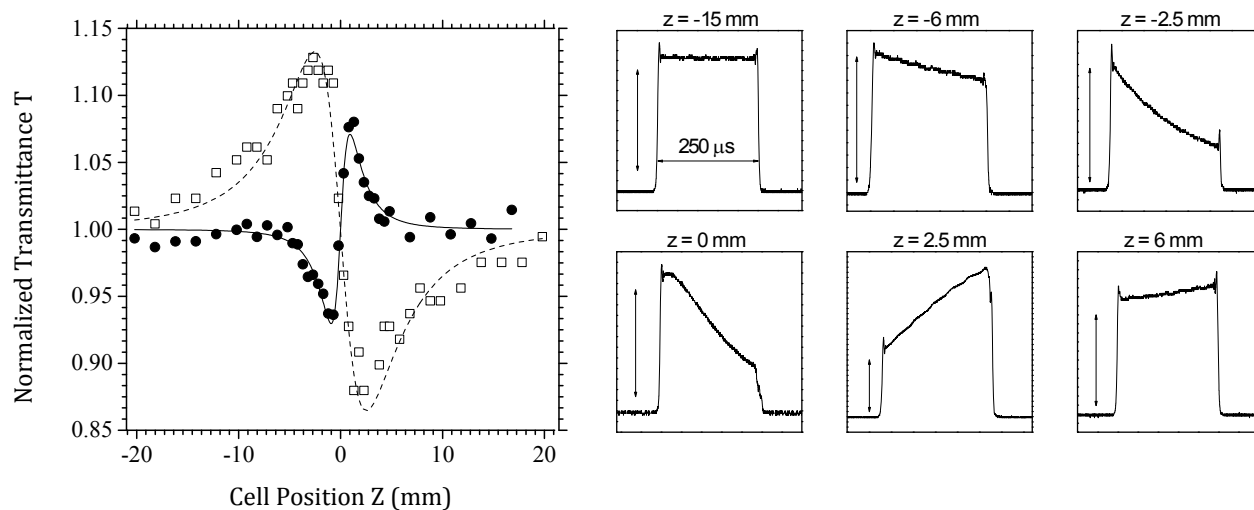
Figure 2. Left: Normalized transmittance as a function of the cell position (z coordinate). Filled points (•) correspond to the normalized transmittance measured immediately after the chopper opening rise time (25 μs) of CS$_2$ ($\Delta\phi_0 = 0.35$), while open points (□) correspond to $7.4 \cdot 10^{-3}$ mole/L of compound **1** in THF ($\Delta\phi_0 = -0.66$) at exactly the same delay of 25 μs. Both traces are measured at 780 nm, at an irradiance of 21 GW/cm^2. The solid line is a theoretical fit, according to Eq. (4). Right: Corresponding oscilloscope traces of compound **1** in THF at different cell positions (z). The vertical arrow represents a signal of 100 mV.

2.2 Nonlinear scattering

The third-harmonic scattering[10] setup (THS) is very similar to a conventional femtosecond hyper-Rayleigh scattering setup, which can be modified easily in order to detect third-order hyperpolarizabilities of sample compounds in solution[11-13]. The main necessary change is to shift the laser wavelength to higher values, because (for example) a Ti-Sapphire laser operating at 800 nm results in the third-harmonic wavelength being situated in the UV part of the spectrum, 267 nm, where optical transparency is very difficult to achieve. Optical parametric oscillators can easily convert femtosecond laser pulses at 800 nm to higher wavelength (1100 nm – 2250 nm).

For a collection of incoherent scatterers, the total scattered intensity at the third harmonic wavelength is equal to[14]:

$$I_{3\omega} = \frac{(3\omega)^4 \pi^2}{9c^2 R^2} f_{3\omega}^2 f_\omega^6 N \langle |\gamma_{THS}|^2 \rangle I_0^3 \tag{6}$$

where $f_\alpha = \dfrac{(n_\alpha^2 + 2)}{3}$ is defined as the Lorentz local field factor at frequency α, N is the number density and I_0 is the intensity at the focal point. $\langle |\gamma_{THS}|^2 \rangle$ Is the isotropic average of the electronic second-hyperpolarizability

tensor, which contains in general 27 unique elements. Symmetry in general will reduce the number of independent tensor elements[14]. The scattering process is a result of purely electronic interactions that do not change the population between occupied and excited states, and as a result occurs almost instantaneously. For multi-component systems, such as solvent (subscript s) and a diluted sample compound (subscript x), Eq. (6) is modified to

$$I_{3\omega} = g \left(N_s \langle |\gamma_{\mathrm{THS},s}|^2 \rangle + N_x \langle |\gamma_{\mathrm{THS},x}|^2 \rangle \right) I_0^3 \qquad (7)$$

All constants are collected in the prefactor g, including experimental unknowns such as collection efficiency and scattering geometry. Eq. (7) has the form of a linear equation $y = a + N_x b$ with intercept $g N_s \langle |\gamma_{\mathrm{THS},s}|^2 \rangle I_0^3$ and slope $g \langle |\gamma_{\mathrm{THS},x}|^2 \rangle I_0^3$. The second-hyperpolarizability of the solute can be determined, completely analogous to the HRS case, by a linear fit of the detected third-harmonic intensity signal and the corresponding number density:

$$\gamma_{\mathrm{THS},x} = \sqrt{b/a\, N_s}\, \gamma_{\mathrm{THS},s} \qquad (8)$$

where we have abbreviated $\sqrt{\langle |\gamma_{\mathrm{THS}}|^2 \rangle} = \gamma_{\mathrm{THS}}$. If the value of the solvent is known, determination of the second-hyperpolarizability of the solute is straightforward.
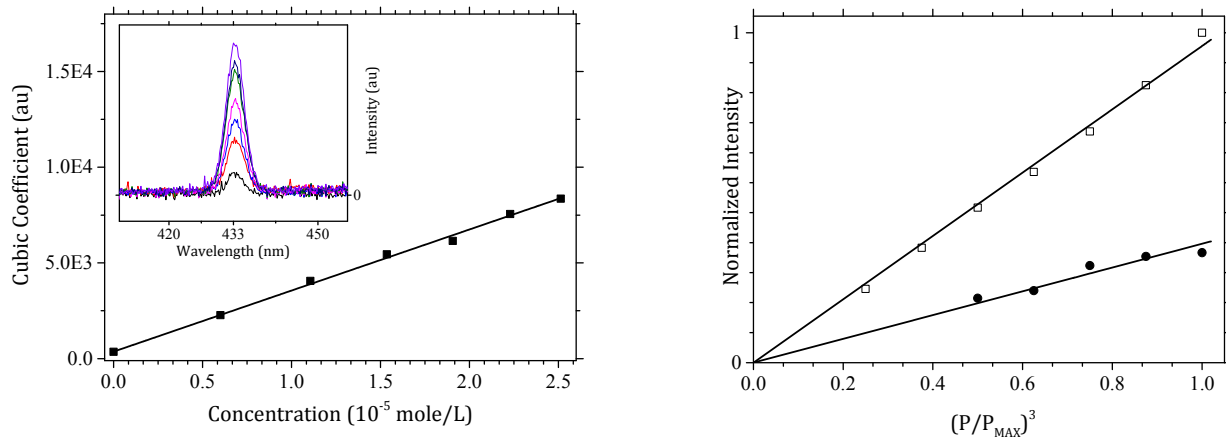
Figure 3. Left: Measured cubic coefficients of compound **1** as a function of the concentration, after correction for absorption of the scattered light using the Lambert-Beer law. The full line is a linear fit, with the intercept fixed at the cubic coefficient of the solvent THF (0 mole/L). The inset shows the recorded spectra of **1**. Right: The measured intensities of $CHCl_3$ (open points) and THF (closed points) show a cubic dependence on the incident relative power (P/P$_{MAX}$). The scale is normalized to the highest intensity of $CHCl_3$.

Eq. (8) assumes that the value of γ of the solvent is known. Due to the nature of the technique, only relative measurements are feasible, as the value of the prefactor g, which contains unknowns such as collection efficiency and scattering geometry, is very impractical to determine accurately. The most straightforward way to calibrate THS measurements is to compare them to third harmonic generation (THG), since the measured tensor elements $\gamma_{ijkl}(-3\omega; \omega, \omega, \omega)$ share the same wavelength dependence. In third harmonic generation, the measured quantity $\langle \gamma_{zzzz} \rangle \equiv \tilde{\gamma}$ is obtained by comparing the THG intensity of the sample in a wedge cell to the third harmonic intensity of quartz, directly related to $\chi^{(3)}_{\mathrm{quartz}}$. To relate THS measurements, we make the assumption that $\gamma_{\mathrm{THS,THF}} \approx \tilde{\gamma}_{\mathrm{THF}}$. In general, one can expect at least the same order of magnitude for these quantities. Multiple

studies[15,16] report THG measurements of the second hyperpolarizabilities at 1907 nm for a large variety of solvents. However, the value of the calibration standard $\chi_{\text{quartz}}^{(3)}$ used[17] changed significantly over the years. At the time of writing, it is now assumed to be approximately a factor of 2.68 lower, a value deemed stable from changing, determined by several independent experimental techniques[18]. Using the most recent calibration standard of $\chi_{\text{quartz}}^{(3)}$ $((1.99 \pm 0.08) \cdot 10^{-22}$ m²V⁻², $(1.42 \pm 0.06) \cdot 10^{-14}$ esu$)$, we obtain $\gamma_{\text{THS,THF}} \approx \tilde{\gamma}_{\text{THF}} = 0.84 \cdot 10^{-36}$ esu $= 1.03 \cdot 10^{-61} \text{C}^4\text{m}^4\text{J}^{-3}$.

If the signals of two different liquids are to be compared, a more detailed analysis is necessary, since the intensity at the beam waist is highly dependent upon the size of the beam waist, which in turn is dependent upon the refractive index of the medium. We now present the detailed procedure to analyze the scattered intensity of different solvents. For a Gaussian beam at radial distance r, axial distance z of the waist and intensity $I(r,z) = \frac{2P_0}{\pi w^2(z)} \exp\left(\frac{-2r^2}{w^2(z)}\right)$, the total scattered third-harmonic intensity originating from a pure liquid (subscript s) is equal to the integral of the whole scattering focal volume:

$$I_{3\omega} = g' \int_0^{2\pi} \int_{-\infty}^{\infty} \int_0^{\infty} \left[\frac{2P_0}{\pi w^2(z)} e^{-2r^2/w^2(z)} \right]^3 r \, dr \, dz \, d\theta \tag{9}$$

$$I_{3\omega} = g' \frac{2P_0^3 z_r}{3w_0^4 \pi} = g' \frac{2P_0^3 n_{s,\omega}}{3w_0^2 \lambda_0} \tag{10}$$

where we have introduced the prefactor $g' = gN_s \langle |\gamma_{\text{THS},s}|^2 \rangle$ and the vacuum wavelength λ_0. Expressing the beam waist as $\theta_s = \frac{\lambda_0}{\pi w_0 n_s}$, and applying Snell's law at the air (subscript a)-liquid interface, $n_a \theta_a \cong n_s \theta_s$, leads to:

$$I_{3\omega} = g' \frac{2\pi^2 P_0^3 n_{s,\omega} n_{a,\omega}^2 \theta_a^2}{3\lambda_0^3} = g' \frac{\pi^2 P_0^3 n_{s,\omega} n_{a,\omega}^2}{6\lambda_0 (f/\#)^2} \tag{11}$$

In the last equality we have used $\theta_a = \frac{1}{2(f/\#)} = \frac{D}{2f}$, where D is the diameter of the lens and f the focal length. In addition to refraction of the fundamental incident beam, the scattered light is also refracted at the air-liquid interface, which introduces an additional factor $n_{a,3\omega}^2 / n_{s,3\omega}^2$. Adding the transmittance (T), a Lambert-Beer correction factor to account for absorption and expanding the factor g', the total formula finally reads:

$$I_{3\omega} \propto \frac{n_{a,3\omega}^2}{n_{s,3\omega}^2} \frac{n_{s,\omega} n_{a,\omega}^2}{(f/\#)^2} T_{3\omega} T_\omega^3 \left(\frac{n_{s,\omega}^2 + 2}{3} \right)^6 \left(\frac{n_{s,3\omega}^2 + 2}{3} \right)^2 \langle |\gamma_{\text{THS},s}|^2 \rangle N_s P_\omega^3 10^{(-3\varepsilon_\omega l C)} \tag{12}$$

The transmittance differences between different solvents usually never exceed 1% and thus can be safely ignored. At longer wavelengths (≥1200 nm), many solvents start absorbing due to the presence of absorption peaks of, in particular, C-H vibration modes and overtones. Visible transparency is usually fine, as long as the third-harmonic wavelength is not less than approximately 300 nm. Incidentally, the refractive indices appearing in Eq. (12) are the same as in HRS[12].

We determined the second hyperpolarizability tensor for the compounds **1-4** (Table 1). Several compounds showed multi-photon induced fluorescence (MPF) (Fig. 4), which necessitated a fitting procedure, such that the narrow, Gaussian THS peak could be extracted from the broad MPF band. The highest value of $2755 \cdot 10^{-36}$ esu ($3411 \cdot 10^{-61}$ C⁴m⁴J⁻³) is more than a factor of 400 times higher than the "benchmark" molecule *trans*-stilbene. Such high values can likely only be explained by the effect of resonance enhancement; indeed, there seems to be a correlation between the magnitude of the γ tensor and the proximity of the low-energy absorption peak to the triple resonance wavelength of 433 nm.
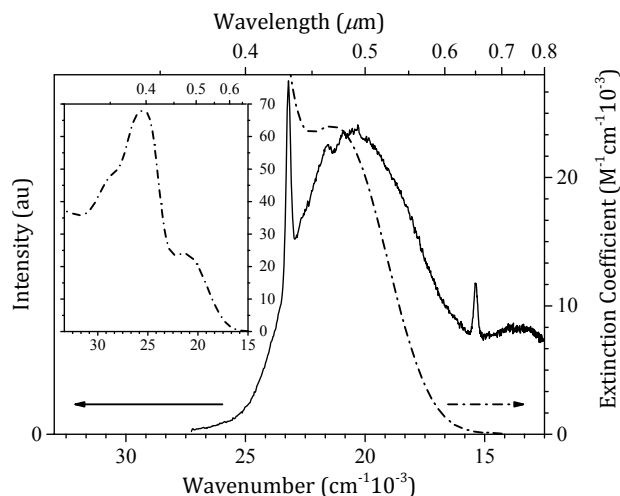
Figure 4. Absorption spectrum of compound **4** $(- \cdot -)$, together with the nonlinear luminescence spectrum $(-)$, at an excitation wavelength of 1300 nm/7692 cm^{-1}. The inset shows the absorption spectrum with an expanded vertical scale. In the luminescence spectrum, one can clearly see the hyper-Rayleigh scattering peak (second-harmonic) at double frequency (650 nm/15 385 cm^{-1}) and the third-harmonic scattering peak at triple frequency (433 nm/23 095 cm^{-1}).

Table 1. Experimental linear optical properties and nonlinear scattering-derived third-order hyperpolarizabilities.

Compound[a]	λ_{MAX} (ε) (nm)(10^4M^{-1}cm^{-1})	$\lvert\gamma_{THS}\rvert$[b] (10^{-36} esu)
trans-[Ru(4-C≡CC$_6$H$_4$NO$_2$)(C≡CPh)(2,3-dppb)$_2$] (**1**)	489 (2.10)	1911
trans-[Ru(4-C≡CC$_6$H$_4$NO$_2$)(4-C≡CC$_6$H$_4$NPh$_2$)(2,3-dppb)$_2$] (**2**)	494 (2.29)	1055
trans-[Ru(4-C≡CC$_6$H$_4$NO$_2$)(4,4',4''-C≡CC$_6$H$_4$C≡CC$_6$H$_4$C≡CC$_6$H$_4$NPh$_2$)(2,3-dppb)$_2$] (**3**)	490 (2.59)	1656
trans-[Ru(4,4'-C≡CC$_6$H$_4$C≡CC$_6$H$_4$NO$_2$)(4,4'-C≡CC$_6$H$_4$C≡CC$_6$H$_4$NPh$_2$)(2,3-dppb)$_2$] (**4**)	471 (2.40)	2755

[a]2,3-dppb = 2,3-bis(diphenylphosphino)butane. [b]The relative experimental error is approximately 15%.

3. CONCLUSION

We have demonstrated the applicability of nonlinear scattering in determining the electronic second hyperpolarizability of ruthenium alkynyl complexes dissolved in tetrahydrofuran. This technique proves to be extremely sensitive in comparison with z-scan, mainly due to different quantities probed: while in z-scan the measured nonlinear refractive index scales linearly with γ, scattering scales with the square of γ, greatly increasing contrast between sample and solvent. This permits the use of extremely low analyte concentrations (up to 10^{-6} mole/L). The increased sensitivity comes at the cost of extra information, as it is only possible to extract the magnitude of the hyperpolarizabiltiy tensor and not its sign. In similar experimental conditions, it was deemed infeasible to extract electronic hyperpolarizabilities with a modified z-scan technique from high repetition rate, femtosecond laser sources, where thermal lensing is problematic. In contrast, nonlinear scattering is inherently a fast process which only depends on the electronic polarization. The effects that interfere with z-scan measurements of high repetition rate laser sources are thus absent. While thermal effects are generally several orders of magnitude higher than their electronic counterparts, only substances possessing the latter property can fulfill the material requirement of high processing speeds in optical devices. The investigated ruthenium alkynyl complexes showed a significant second hyperpolarizability $\lvert\gamma\rvert$, ranging from 1.1 - 2.8 · 10^{-33}esu, and comparable to fullerene C$_{60}$ in thin films[19].

4. EXPERIMENTAL

4.1 Synthesis

The synthesis and characterization of the ruthenium complexes will be reported elsewhere[20].

4.2 General experimental info

All nonlinear optical experiments were conducted using a high frequency (80 MHz), femtosecond pulsed InSight DS+ laser, capable of producing a beam devoid of significant intensity variations, both long term and short term ($< 1\%$). Correcting for intensity fluctuations was therefore not done. The pulse full width at half maximum (FWHM) was measured to be 128 fs at 850 nm (autocorrelator model 409-8 deployed with an etalon of 1560 fs).

4.3 Z-scan

The detailed layout of a z-scan setup can be found elsewhere [4]. An S-polarized laser beam was first spatially filtered in order to achieve a near perfect TEM_{00} mode Gaussian beam. An achromatic lens subsequently focused the light onto a 1 mm path length fused silica cuvette placed on a translation stage. The transmittance of the closed aperture scan was measured by a PIN photodiode (Hamamatsu S2381, active area 0.03 mm^2), positioned approximately 50 cm away from the z_0 position of the cuvette. A PIN photodiode with larger active area (Hamamatsu S1722-02, active area 13.2 mm^2), in conjunction with a focusing lens, was used for the open aperture scan. The on-axis irradiance at z_0 (I_0) was equal to 21 GW/cm^2 at 780 nm. Measurement of fast, electronic nonlinearities was done by inserting a chopper immediately after the pinhole of the spatial filter [6]. Time dependent transmittances were measured by connecting the output voltage of the closed aperture photodiode to a Tektronix TDS 3034B, operated at 20 MHz bandwidth and a sample averaging of 128.

4.4 Nonlinear scattering

We used a slightly modified version of the hyper-Rayleigh scattering (HRS) setup [21][12] for the third-harmonic scattering experiments. Following an achromatic half-wave plate and polarizer combination used for intensity variation, the S-polarized beam was subsequently, without any spatial filtering, focused into a 10 mm path length cuvette made of fused silica (Spectrosil) by an aspheric lens (f/2). The spacing between the wall of the cuvette and the laser focal point was approximately 1 mm. The scattered light at a 90° angle was collimated by a 1" achromatic, aspheric condenser lens, passed through a dove prism rotated 45° to rotate the image 90°, expanded to a 2" beam diameter, and finally focused onto the entrance slit of a slit imaging spectrometer (Bruker 500 is/sm). The spectra were recorded by an EMCCD camera (Andor Solis model iXon Ultra 897), but the EM mode was not used due to an abundance of signal. Typical recording times ranged from 1 s to 15 s. The average power used was ≈ 550 mW at 1300 nm. Before conducting any measurements, it was necessary to pass all samples through 0.45 μm filters (Millex, Millipore) to remove any dust or small particles, which can interfere with the measurement. All compounds were measured in THF, at concentrations of $\approx 10^{-5}$ mole/L.

ACKNOWLEDGEMENTS

REFERENCES

[1] Fisher, R., Optical Phase Conjugation, Academic (1983).

[2] Gibbs, H. M., Controlling Light with Light, Academic Press (1985).

[3] Bowden, C. M., Giftan, M.., Robl, H. R., Optical Bistability, Plenum (1981).

[4] Sheik-Bahae, M., Said, A. A., Wei, T. H., Hagan, D. J.., Van Stryland, E. W., "Sensitive Measurement of Optical Nonlinearities Using a Single Beam," IEEE J. Quantum Electron. **26**(4), 760–769 (1990).

[5] Chapple, P. B., Staromlynska, J., Hermann, J. A., McKay, T. J.., McDuff, R. G., "Single-Beam Z-Scan: Measurement Techniques and Analysis," J. Nonlinear Opt. Phys. Mater. **6**(3), 251–293 (1997).

[6] Falconieri, M.., Salvetti, G., "Simultaneous measurement of pure-optical and thermo-optical nonlinearities induced by high-repetition-rate, femtosecond laser pulses: Application to CS2," Appl. Phys. B Lasers Opt. **69**(2), 133–136 (1999).

[7] Falconieri, M., "Thermo-optical effects in Z -scan measurements using high-repetition-rate lasers," J. Opt. A Pure Appl. Opt. **1**(6), 662–667 (1999).

[8] Couris, S., Renard, M., Faucher, O., Lavorel, B., Chaux, R., Koudoumas, E.., Michaut, X., "An experimental investigation of the nonlinear refractive index (n2) of carbon disulfide and toluene by spectral shearing interferometry and z-scan techniques," Chem. Phys. Lett. **369**(3-4), 318–324 (2003).

[9] Sheldon, S. J., Knight, L. V., Thorne, J. M., "Laser-induced thermal lens effect: a new theoretical model.," Appl. Opt. **21**(9), 1663–1669 (1982).

[10] Van Steerteghem, N., Clays, K., Verbiest, T.., Van Cleuvenbergen, S., manuscript in preparation.

[11] Olbrechts, G., Munters, T., Clays, K.., Persoons, A., "High-frequency demodulation of multiphoton fluorescence for hyper-Rayleigh scattering in solution," Broadband Opt. Networks Technol. An Emerg. Reality/Optical MEMS/Smart Pixels/Organic Opt. Optoelectron. 1998 IEEE/LEOS Summer Top. Meet., III/33 – III/34 (1998).

[12] Campo, J., Desmet, F., Wenseleers, W.., Goovaerts, E., "Highly sensitive setup for tunable wavelength hyper-Rayleigh scattering with parallel detection and calibration data for various solvents.," Opt. Express **17**(6), 4587–4604 (2009).

[13] Yamada, T.., Mashiko, S., "Third-Order Hyper-Rayleigh Scattering in an Azobenzene Dye Solution," Jpn. J. Appl. Phys. **39**(10B), L1060 (2000).

[14] Alexiewicz, W., Ozgo, Z.., Kielich, S., "Spectral theory of third-harmonic light scattering by molecular liquids," Acta Phys. Pol. A **48**, 243–252 (1975).

[15] Kajzar, F.., Messier, J., "Third-harmonic generation in liquids," Phys. Rev. A **32**(4), 2352–2363 (1985).

[16] Meredith, G. R., Buchalter, B.., Hanzlik, C., "Third-order susceptibility determination by third harmonic generation. II," J. Chem. Phys. **78**(3), 1543–1551 (1983).

[17] Meredith, G. R., "Cascading in optical third-harmonic generation by cyrstalline quartz," Phys. Rev.

B **24**(10), 5522–5532 (1981).

[18]   Bosshard, C., Gubler, U., Kaatz, P., Mazerant, W.., Meier, U., "Non-phase-matched optical third-harmonic generation in noncentrosymmetric media: Cascaded second-order contributions for the calibration of third-order nonlinearities," Phys. Rev. B **61**(16), 10688–10701 (2000).

[19]   Nalwa, H. S., "Organic Materials for Third-Order Nonlinear Optics," Adv. Mater. **5**(5), 341–358 (1993).

[20]   Shah, N. A. A., Moxey, G. J., Morshedi, M., Wang, G., Cifuentes, M. P., Van Steerteghem, N., Van Cleuvenbergen, S., Verbiest, T., Clays, K., et al., manuscript in preparation.

[21]   Clays, K.., Persoons, A., "Hyper-Rayleigh scattering in solution," Phys. Rev. Lett. **66**(23), 2980–2983, American Physical Society (1991).